

# Half-metallic Surface States and Topological Superconductivity in $\text{NaCoO}_2$

Hongming Weng<sup>1</sup>, Gang Xu<sup>1</sup>, Haijun Zhang<sup>2</sup>,

Shou-Cheng Zhang<sup>2,3</sup>, Xi Dai<sup>1\*</sup> and Zhong Fang<sup>1†</sup>

<sup>1</sup> *Beijing National Laboratory for Condensed Matter Physics,  
and Institute of Physics, Chinese Academy of Sciences, Beijing 100190, China;*

<sup>2</sup> *Department of Physics, McCullough Building,  
Stanford University, Stanford, CA 94305-4045; and*

<sup>3</sup> *Center for Advanced Study, Tsinghua University, Beijing, 100084, China*

(Dated: January 14, 2013)

## Abstract

Based on the first-principles calculations, we predict a novel half-metallic surface state in layered bulk insulator  $\text{NaCoO}_2$ , with tunable surface hole concentration. The half-metallic surface has a single fermi surface with a helical spin texture, similar to the surface state of topological insulators, but with the key difference of time reversal symmetry breaking in the present case. We propose realization of topological superconductivity and Majorana fermions when the half-metallic surface states are in proximity contact with a conventional superconductor.

---

\*Electronic address: daix@aphy.iphy.ac.cn

†Electronic address: zfang@aphy.iphy.ac.cn

The possibility of realizing Majorana fermions in condensed matters as emergent excitations has stimulated great current interest. Majorana fermions are particles which are their own antiparticles [1]. They constitute only half of a usual fermion, and obey the non-Abelian statistics [2], which is the key ingredient for the fault-tolerant topological quantum computation [3]. The Majorana states associated with zero energy mode have been predicted to exist in various systems [2, 4–12], nevertheless, their experimental realizations remain challenging due to the requirements of extreme conditions such as strong magnetic field, low temperature, or ultra-clean samples. In this letter, we will show that NaCoO<sub>2</sub>/superconductor heterostructure is a new and simple platform for realizing such exotic states.

The simplest Majorana bound state is associated with a vortex core or edge in a two-dimensional (2D) topological  $p_x + ip_y$  superconductor [5, 6], which has a full pairing gap in the bulk but with gapless chiral edge states (which consists of Majorana fermions). Unfortunately, such topological superconductors are very rare in nature, this leads to the proposals of possible “induced”  $p_x + ip_y$  order parameter through the proximity effect, particularly for materials in contact with the simplest  $s$ -wave superconductors [7–12]. The proposal by Fu and Kane [7] is to use the surface state of topological insulators [13–15], where the spin degeneracy is removed and yet strong proximity effect can be expected due to the characteristic helical spin texture of Dirac-type surface state. The experimental setting can be in principles obtained from laboratory, however, since most known three-dimensional topological insulators [15–18] up to now are not good bulk insulators and important surface states may overlap with bulk states, experiments have to wait for development of well-controlled clean samples. It was proposed recently that semiconductor quantum wells with Rashba type SOC in proximity to  $s$ -wave superconductor will produce similar effect [8–11]. This may lower the experimental threshold, since well-controlled samples are available nowadays. Both proposals are encouraging, while experimental obstacles still remain. First, and most importantly, magnetic insulating layers or strong external magnetic field are required to break the time reversal symmetry, which is not easy to implement experimentally; second, the Fermi surfaces in both cases are too small, and fine control of chemical potential is difficult for semiconductors in contact with a superconductor.

To avoid the complication required by breaking time reversal symmetry (such as the usage of magnetic insulating layers or magnetic field), the most natural way is to start from a magnetic compound, rather than non-magnetic topological insulators or semiconductor

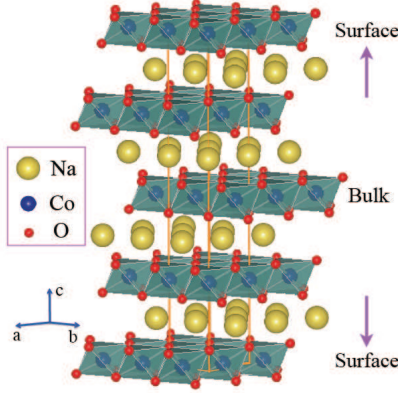


FIG. 1: (Color online) The structure of  $\text{NaCoO}_2$  slab consisting of 5 unit layers. After structure optimization, the surface Co-O bond-lengths are slightly modified (by  $0.07\text{\AA}$ ).

quantum wells. On the other hand, however, the following ingredients have to be satisfied over a wide energy or doping regime, in order to induce the  $p_x + ip_y$  superconductivity through proximity effect: (1) two dimensional metal with a single (or an odd number of) Fermi surface; (2) strong enough helical spin texture arising from spin-orbit coupling (SOC). Those conditions all together suggest that a 2D single band half-metal materials with strong enough SOC will be the best candidate [12, 19]. Following this strategy, we propose in this work that  $\text{NaCoO}_2$  is such a unique compound, which satisfies all those conditions simultaneously.

Bulk  $\text{Na}_x\text{CoO}_2$  is a well known layered compound crystallizing in planar triangle lattice with Co atom coordinated by oxygen octahedrally (Fig.1). The Na atoms are interpolated between  $\text{CoO}_2$  layers, and its concentration  $x$  can be systematically tuned, resulting in complex magnetic and electronic phase diagram [20]. In particular, the unconventional superconductivity around  $x=0.35$  [21], and the layered antiferromagnetic (AF) phase around  $x > 0.65$  [22–24], have drawn lots of attentions. For our purpose, however, we consider the stoichiometry  $\text{NaCoO}_2$  (i.e.  $x=1.0$ ) and its surface state.

$\text{NaCoO}_2$  single crystal (with  $R\bar{3}m$  symmetry) is experimentally available [25], and it is a simple band insulator with band gap more than  $1.0\text{eV}$  [25]. Its bulk insulating behavior has been indicated by transport [26] and NMR [27] measurements. Electronically, the Co- $3d$  states splits into  $t_{2g}$  and  $e_g$  manifolds under oxygen octahedron crystal field, and all  $t_{2g}$  states are fully occupied (by 6 electrons) in the case without Na deficiency (corresponding to nominal  $\text{Co}^{3+}$  case), resulting in an band gap between  $t_{2g}$  and  $e_g$  [25, 27]. The layered crystal

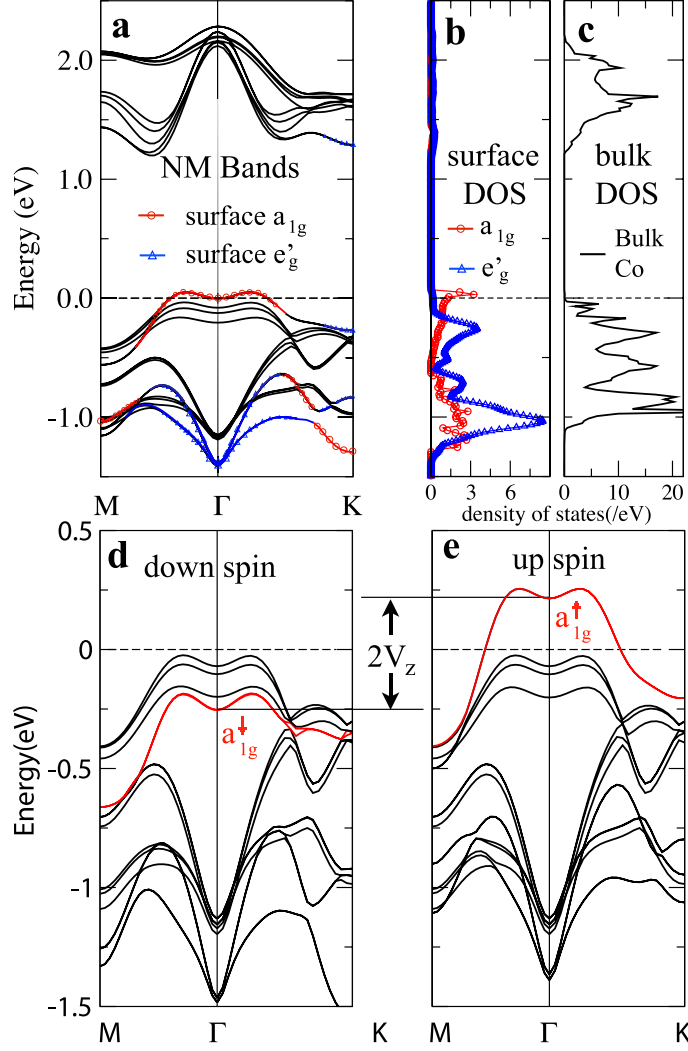


FIG. 2: (Color online) The calculated band structure and density of state (DOS) for NaCoO<sub>2</sub> slab with surface hole concentration  $y=0.3$ . (a) The band structure of non-magnetic (NM) state. The projections to the  $a_{1g}$  and  $e'_g$  states of surface Co are indicated as red circle and blue triangle, respectively. (b) and (c) The corresponding DOS for the surface and bulk Co sites, respectively. The character of insulating bulk with metallic surface is seen. (d) and (e) The spin-resolved band structure of ferromagnetic state with the  $V_z$  defined as the exchange splitting of surface  $a_{1g}$  state.

structure guarantees that samples can be easily cleaved (Fig.1), and two kinds of terminations, with or without top-most Na layer, may be realized. Nevertheless, since the top-most Na<sup>1+</sup> ions are highly mobile, its concentration can be tuned depending on experimental conditions, resulting in surface hole doping (indicated as  $y$ ) but without modifying the surface structure (the CoO<sub>2</sub> layer) significantly. In the extreme case, if all top-most Na are absent,

0.5 hole will be introduced (i.e.  $y=0.5$ ). We study the (001) surface of  $\text{NaCoO}_2$  by using the first-principles calculations based on the plane-wave ultra-soft pseudopotential method, and the generalized gradient approximation (GGA) for the exchange-correlation functional. A slab consisting of five  $\text{NaCoO}_2$  unit layers thickness (Fig.1) and 20 Å vacuum region is used for the surface study, and the SOC is included from the fully relativistic pseudopotential. The cutoff energy for wave-function expansion is 30 Ry, and we use  $12 \times 12$  k-points mesh for the Brillouin zone sampling. The calculations are well converged with respect to above settings. The calculations are further supplemented by the LDA+Gutzwiller method [28], in which the density functional theory is combined with the Gutzwiller variational approach such that the orbital fluctuation and kinetic renormalization coming from correlation are all self-consistently treated.

By optimizing the surface (slab) structure without top-most Na layer, our calculations confirm that the surface  $\text{CoO}_2$  layer remain well defined with only slightly (about 0.07Å) modification of surface Co-O bond length (see Fig.1). Another key result obtained from this calculation is that the hole only goes into the surface  $\text{CoO}_2$  layer, while keeping all other  $\text{CoO}_2$  layers inside the bulk insulating. There is only one band cross the Fermi level (Fig.2), which comes from one of the  $t_{2g}$  states of the top-most Co sites, while all other  $\text{Co-}t_{2g}$  states inside the bulk are fully occupied. It is therefore effectively a system with insulating bulk but metallic surface, similar to topological insulators [13–15]. The key difference lies in the fact that the surface state considered in this work breaks the time reversal symmetry, in contrast to the case of topological insulators. In reality, the surface hole doping can be tuned by modifying the surface Na concentration, by interface charge transfer, or simply by gating. In the case of proximity effect with a superconductor, such surface doping can naturally arise since many  $s$ -wave superconductors, like Al, Pb or Nb, are simple metals. In such case, the insulating  $\text{NaCoO}_2$  bulk can even serve as substrate simultaneously. In the following discussions, we will therefore neglect the top-most Na atoms and use the virtual crystal approximation to simulate the surface doping effect.

Fig.3 shows the magnetic properties of the  $\text{NaCoO}_2$  surface as function of hole concentration  $y$ . The spin polarization is energetically favored for all hole concentration ( $0.5 < y < 0$ ), in close analogy to the layered AF phase of  $\text{Na}_x\text{CoO}_2$  bulk ( $x \sim 0.75$ ) [20, 22, 29], where each  $\text{CoO}_2$  layer (with  $\sim 0.25$  hole) orders ferromagnetically and the in-plane ferromagnetism contributes mostly to the energy gain with relatively weak inter-layer AF coupling. The sta-

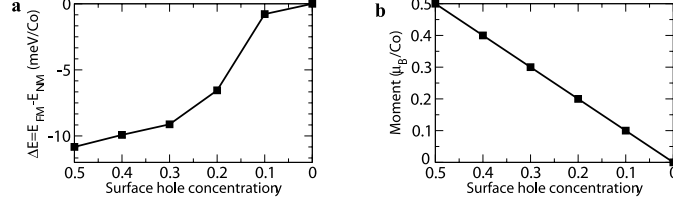


FIG. 3: (Color online) The calculated magnetic properties of NaCoO<sub>2</sub> surface as function of surface hole concentration  $y$ . (a) The stabilization energy of ferromagnetic (FM) state with respect to non-magnetic (NM) state. (b) The magnetic moment of surface CoO<sub>2</sub> layer.

bilization of ferromagnetism at NaCoO<sub>2</sub> surface can be intuitively understood from Stoner instability (also similar to the discussion addressed for the layered AF bulk Na<sub>0.75</sub>CoO<sub>2</sub> [29]). Due to the elongation of oxygen octahedra around Co sites along  $c$ -axis, the Co- $t_{2g}$  states will further split into  $a_{1g}$  and  $e'_g$  manifolds, with  $a_{1g}$  higher in energy. The  $a_{1g}$  state has mostly  $3d_{3z^2-r^2}$  orbital character (with  $z$  defined along  $c$ ), whose in-plane dispersion is relatively weak and “M” shaped as observed in ARPES experiment [30]. As shown in Fig.2(a), the wide region of nearly-flat-bands around the valence band maximum will produce a sharp DOS peak near the Fermi level (see Fig.2(b)), which leads to the Stoner instability, and favors the ferromagnetic (FM) ground state for the surface. This mechanism is further supported by the electronic structure of FM solution (Fig.2(c) and (d)), where only the  $a_{1g}$  state is strongly spin-polarized and the polarization of  $e'_g$  states is small. In the FM state, the spin-polarization is strong enough to make the top-most CoO<sub>2</sub> layer a half-metal, as shown in Fig.2 and Fig.3, where the calculated magnetic moment exactly equals to the number of holes. There is only one spin-channel of  $a_{1g}$  state crossing the Fermi level, resulting in a half-metallic surface state with single sheet of Fermi surface.

We have to be aware of the effect of electron correlation beyond the generalized gradient approximation (GGA) for the exchange-correlation potential. The LDA+Gutzwiller method [28] has been shown to be a powerful tool to take into account the correlation effect, and reproduce correctly the magnetic phase diagram of bulk Na <sub>$x$</sub> CoO<sub>2</sub> [29]. We have supplemented the LDA+Gutzwiller calculations for the surface, and find that the surface ferromagnetism is further stabilized (by about 8meV/surface Co for  $y=0.3$ ). In fact, in the study for the bulk Na <sub>$x$</sub> CoO<sub>2</sub> ( $x > 0.6$ ), both GGA and LDA+Gutzwiller give qualitatively the same result, well compared to experiments [29]. The AF state of bulk Na <sub>$x$</sub> CoO<sub>2</sub> was

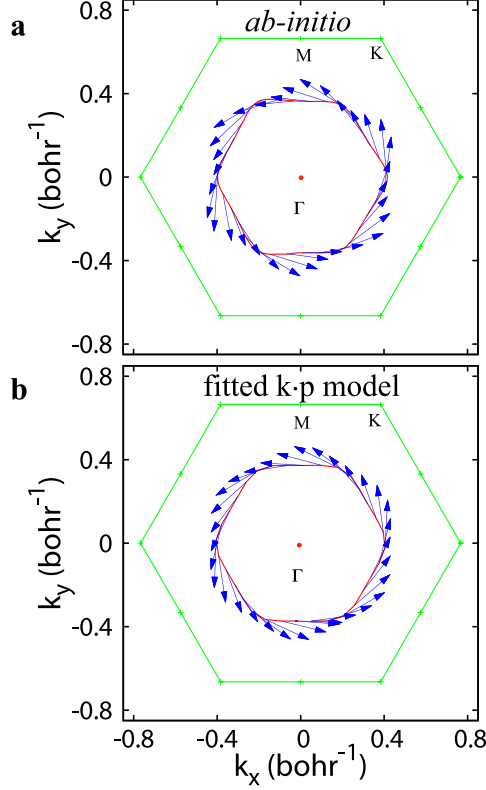


FIG. 4: (Color online) The Fermi surface and the helical spin texture of  $\text{NaCoO}_2$  surface (for  $y=0.3$ ) obtained from (a) first-principles calculations, and (b) evaluation of effective  $k \cdot p$  model (Eq.1, see text part) with parameter  $A=0.28 \text{ eV}\text{\AA}^2$ ,  $B=0.53 \text{ eV}\text{\AA}^6$ ,  $C=-2.4 \text{ eV}\text{\AA}^6$ ,  $\alpha=-0.066 \text{ eV}\text{\AA}$ ,  $V_z=0.22\text{eV}$ . The in-plane components of spin are indicated as arrowed lines, while the perpendicular component (pointing to out-of-plane) is not shown.

observed for  $x > 0.65$  with maximum  $T_c$  around 25K for  $x \sim 0.8$ , the layered ordering with spin orientation perpendicular to the plane was confirmed by neutron experiments [23, 24], and its half-metallicity of in-plane electronic structure is also supported by the ARPES measurements [31, 32]. Considering the layered nature and the similarity between the bulk AF phase and the surface, we conclude that a single band half metal can be realized at  $\text{NaCoO}_2$  surface with tunable hole concentration.

Turning on the the SOC, the up and down spin bands will couple, while the characteristic single sheet of Fermi surface still remains. In the presence of a surface, the asymmetrical surface potential will produce the Rashba type SOC (which is automatically included in the first-principles calculations). It turns out that the Rashba SOC plays important roles, resulting in the in-plane spin component, which has helical spin texture for the states at

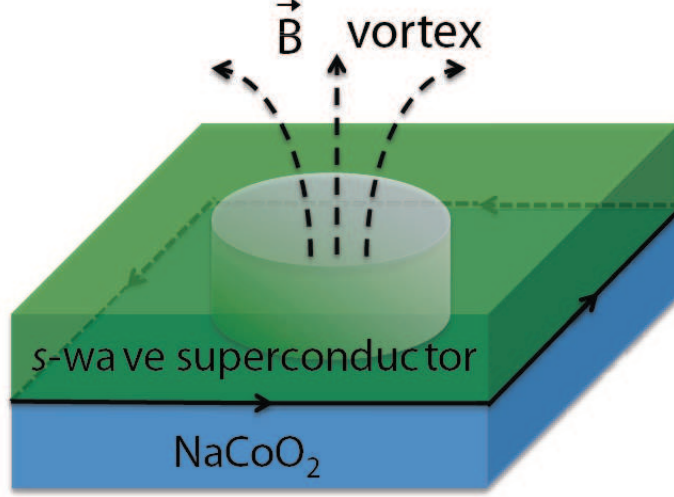


FIG. 5: (Color online) The schematic picture for the NaCoO<sub>2</sub>/s-wave superconductor heterostructure where Majorana bound state is associated with the vortex core. The chiral Majorana edge state is also expected at the edge of interface.

Fermi level (see Fig.4). The in-plane component is actually rather strong, and contribute to more than 10% of the total moment from our first-principles calculations. Considering the single  $a_{1g}$  state of NaCoO<sub>2</sub> surface and the 3-fold rotation symmetry, an effective surface Hamiltonian can be constructed as,

$$H_0 = \sum_{\mathbf{k}} [\xi(\mathbf{k}) + V_z \sigma_z + \alpha(k_y \sigma_x - k_x \sigma_y)]. \quad (1)$$

where  $\xi(\mathbf{k}) = Ak_+k_- + B(k_+^6 + k_-^6) + C(k_+^3k_-^3)$  (with  $k_{\pm} = k_x \pm ik_y$ ) gives the non-spin-polarized band structure,  $V_z \sigma_z$  is the exchange splitting, and the last term is the Rashba type SOC due to the surface. Evaluating the eigen values  $\epsilon(\mathbf{k}) = \xi(\mathbf{k}) \pm \sqrt{V_z^2 + \alpha^2 \mathbf{k}^2}$  with the parameters given in the caption of Fig.4, the Fermi surface and its helical spin texture can be well reproduced (Fig.4(b)). Please note the hole type carrier and the negative sign of Rashba coupling  $\alpha$  in our present case.

When the NaCoO<sub>2</sub> surface comes into contact with an s-wave superconductor, a pairing term  $H_{\Delta} = \sum_{\mathbf{k}} [\Delta c_{\mathbf{k}\uparrow}^{\dagger} c_{\mathbf{k}\downarrow}^{\dagger} + h.c.]$  will be generated by the proximity effect, and the full Hamiltonian reads  $H = H_0 + H_{\Delta}$ , which has been carefully studied previously [8–11, 19]. The dominant pairing channel should have the spin polarized  $p_x + ip_y$  symmetry, whose order parameter is given as  $\Delta_P^+(\mathbf{k}) = \frac{-\alpha k}{\sqrt{(V_z^2 + \alpha^2 k^2)}} \frac{k_y + ik_x}{k} \Delta$ . In the limit of large  $V_z$ , following Ref. [9], the superconducting gap can be estimated as,



$$E_g = \sqrt{\frac{2m^*\alpha^2}{V_z}(1 + \frac{\mu}{V_z})}\Delta \approx 0.22\Delta, \quad (2)$$

which is sizable. Here we use the parameters, effective mass  $m^*=5m_0$ ,  $\alpha = -0.066\text{eV}\text{\AA}$ , and  $V_z=0.22\text{eV}$ , obtained from our first principles calculations. The size of  $\Delta$  is determined by the superconducting gap of  $s$ -wave superconductor and its interface coupling (hopping) with  $\text{NaCoO}_2$  side.

Once the  $p_x + ip_y$  superconductivity is realized through proximity effect, the Majorana bound states associated with the vortex core will be expected [7, 8, 19]. The schematic experimental setting for the detection of Majorana fermions is shown in Fig.5, where the absence of magnetic insulating layer and/or magnetic field is the essential difference compared to earlier proposals [7–9]. In additional, due to the broken time reversal symmetry (different from Fu and Kane’s proposal [7]), a chiral Majorana edge state should exist at the interface (Fig.5). Since the single band half-metallic character of  $\text{NaCoO}_2$  surface can be realized in a large energy window (of about  $0.2\text{eV}$ ), the fine tuning of chemical potential is not necessary. The large Fermi surface size and the high carrier density should be also helpful for sizable proximity effect, against the possible localization due to disorders. Among several possible choices of the superconductor, it is particularly interesting to consider the  $\text{Na}_x\text{CoO}_2$  superconductor with  $x$  around 0.35 [20, 21], since the lattice structures are well matched. The  $\text{NaCoO}_2/s$ -wave superconductor heterostructure, therefore, provide us a new and simple platform for realizing topological superconductivity and Majorana fermion bound states. This work can be generalized in several directions. Similar predictions can be also made for AF  $\text{Na}_x\text{CoO}_2$  ( $x > 0.65$ ) thin film with odd number of layers (which contribute to odd number of Fermi surfaces), or for  $\text{LiCoO}_2$ , which has the same crystal and electronic structure as  $\text{NaCoO}_2$  [33].

We acknowledge the supports from NSF of China and that from the 973 program of China (No.2007CB925000, No.2010CB923000), the US NSF under grant numbers DMR-0904264, and the Keck Foundation.

- 
- [1] See, for example, F. Wilczek, Nat. Phys. **5**, 614 (2009), and references therein.
  - [2] C. Nayak, S. H. Simon, A. Stern, M. Freedman, and S. Das Sarma, Rev. Mod. Phys. **80**, 1083 (2008).
  - [3] A. Kitaev, Ann. Phys. (NY), **303**, 2 (2003).
  - [4] M. Greiter, X. G. Wen, and F. Wilczek, Nucl. Phys. B **374**, 567 (1992).
  - [5] N. Read and D. Green, Phys. Rev. B **61**, 10267 (2000).
  - [6] S. Das Sarma, C. Nayak, and S. Tewari, Phys. Rev. B **73**, 220502 (R) (2006).
  - [7] L. Fu and C. L. Kane, Phys. Rev. Lett. **100**, 096407 (2008).
  - [8] J. D. Sau, R. M. Lutchyn, S. Tewari, and S. Das Sarma, Phys. Rev. Lett. **104**, 040502 (2010).
  - [9] J. Alicea, Phys. Rev. B **81**, 125318 (2010).
  - [10] P. A. Lee, e-print arXiv:0907.2681.
  - [11] A. C. Potter and P. A. Lee, Phys. Rev. B **83**, 094525 (2011).
  - [12] M. Duckheim and P. W. Brouwer, Phys. Rev. B **83**, 054513 (2011).
  - [13] C. L. Kane and E. J. Mele, Phys. Rev. Lett. **95**, 146802 (2005).
  - [14] B. A. Bernevig and S. C. Zhang, Phys. Rev. Lett. **96**, 106802 (2006).
  - [15] H. J. Zhang, C.-X. Liu, X.-L. Qi, X. Dai, Z. Fang and S.-C. Zhang, Nat. Phys. **5**, 438 (2009).
  - [16] D. Hsieh, D. Qian, L. Wray, Y. Xia, Y. S. Hor, R. J. Cava, and M. Z. Hasan, Nature (London) **452**, 970 (2008).
  - [17] Y. Xia, D. Qian, D. Hsieh, L. Wray, A. Pal, H. Lin, A. Bansil, D. Grauer, Y. S. Hor, R. J. Cava, and M. Z. Hasan, Nat. Phys. **5**, 398 (2009).
  - [18] Y. L. Chen, J. G. Analytis, J.-H. Chu, Z. K. Liu, S.-K. Mo, X.-L. Qi, H.-J. Zhang, D.-H. Lu, X. Dai, Z. Fang, S.-C. Zhang, I.-R. Fisher, Z. Hussain, and Z.-X. Shen, Science **325**, 178 (2009).
  - [19] S. B. Chung, H.-J. Zhang, X.-L. Qi, and S.-C. Zhang, e-print arXiv:1011.6422.
  - [20] M. L. Foo, Y. Wang, S. Watauchi, H.-W. Zandbergen, T. He, R. J. Cava, and N. P. Ong, Phys. Rev. Lett. **92**, 247001 (2004).
  - [21] K. Takada, H. Sakurai, E. Takayama-Muromachi, F. Izumi, R. A. Dilanian, and T. Sasaki, Nature (London) **422**, 53 (2003).
  - [22] J. Sugiyama, H. H. Brewer, E. J. Ansaldo, H. Itahara, T. Tani, M. Mikami, Y. Mori, T. Sasaki,

- S. Hébert, and A. Maignan, Phys. Rev. Lett. **92**, 017602 (2004).
- [23] S. P. Bayrakci, I. Mirebeau, P. Bourges, Y. Sidis, M. Enderle, J. Mesot, D. P. Chen, C. T. Lin, and B. Keimer, Phys. Rev. Lett. **94**, 157205 (2005).
- [24] L. M. Helme, A. T. Boothroyd, R. Coldea, D. Prabhakaran, D. A. Tennant, A. Hiess, and J. Kulda, Phys. Rev. Lett. **94**, 157206 (2005).
- [25] Y. Takahashi, Y. Gotoh, and J. Akimoto, J. Solid State Chem. **172**, 22 (2003).
- [26] S. Kikkawa, S. Miyazaki, and M. Koizumi, J. Solid State Chem. **62**, 35 (1986).
- [27] C. de Vaulx, M.-H. Julien, C. Berthier, M. Horvatić, P. Bordet, V. Simonet, D.-P. Chen, and C.-T. Lin, Phys. Rev. Lett. **95**, 186405 (2005).
- [28] X. Y. Deng, X. Dai, Z. Fang, Europhys. Lett. **83**, 37008 (2008).
- [29] G. T. Wang, X. Dai, Z. Fang, Phys. Rev. Lett. **101**, 066403 (2008).
- [30] T. Arakane, T. Sato, T. Takahashi, T. Fujii, and A. Asamitsu, New J. Phys. **13**, 043021 (2011)
- [31] J. Geck, S. V. Borisenko, H. Berger, H. Eschrig, J. Fink, M. Knupfer, K. Koepernik, A. Koitzsch, A. A. Kordyuk, V. B. Zabolotnyy, and B. Büchner, Phys. Rev. Lett. **99**, 046403 (2007).
- [32] M. Z. Hasan, Y.-D. Chuang, D. Qian, Y. W. Li, Y. Kong, A. Kuprin, A. V. Fedorov, R. Kimmerling, E. Rotenberg, K. Rossnagel, Z. Hussain, H. Koh, N. S. Rogado, M. L. Foo, and R. J. Cava, Phys. Rev. Lett. **92**, 246402 (2004).
- [33] Y. Takahashi, Y. Totoh, J. Akimoto, S. Mizuta, K. Tokiwa, and T. Watanabe, J. Solid State Chem. **164**, 1 (2002).